UTILIZING STRESS-BASED FAILURE CRITERIA FOR PREDICTION OF CURING INDUCED DAMAGE IN 3D WOVEN COMPOSITES

Igor Tsukrov[1], Borys Drach[2], Andrew Drach [3], and Todd Gross[1]

[1] Mechanical Engineering, University of New Hampshire, Durham NH, USA, igor.tsukrov@unh.edu
[2] Mechanical & Aerospace Engineering, New Mexico State University, Las Cruces NM, USA
[3] Institute for Computational Engineering & Sciences, University of Texas at Austin, Austin TX, USA

Keywords: Woven composites, Failure criteria, Curing, Finite elements, Damage propagation

ABSTRACT

There are several possible mechanisms of failure of glassy polymers that can be activated by different states of stress in the material. They are reflected in the various failure criteria used to predict initiation of damage in the polymer based on the components of stress tensor. We investigated the applicability of several popular failure criteria (the von Mises, the Drucker-Prager, the parabolic stress, and the dilatational strain energy density) to predict processing-induced damage due to cooling after curing observed in 3D woven composites with high level of through-thickness reinforcement.

We developed high-fidelity mesoscale finite element models of orthogonally reinforced carbon/epoxy composites and predicted their response to the uniform temperature drop from the curing to room temperature. Comparison of the simulation results with the X-ray computed microtomography indicates that matrix failure caused by the difference in thermal expansion coefficients of carbon fiber and epoxy resin is well predicted by the dilatational strain energy criterion. Initiation and propagation of this failure was numerically investigated using sequential deactivation of elements exceeding the allowable equivalent stress.

1 INTRODUCTION

3D woven composites possess superior mechanical properties compared to 2D woven composite laminates due to continuous reinforcement in all three dimensions resulting in high strength and additional fatigue resistance under multiaxial loading. However, some 3D woven composite material systems are prone to matrix microcracking during manufacturing. Figure 1 illustrates microcracks that developed in a 3D woven carbon/epoxy composite with significant through-thickness reinforcement after matrix curing at elevated temperature. We assume that the major factor in process-induced microcracking of woven composites is the residual stress due to mismatch of thermal expansion coefficients (CTEs) of carbon fibers and epoxy matrix developing when completely cured matrix cools from the curing to room temperature.

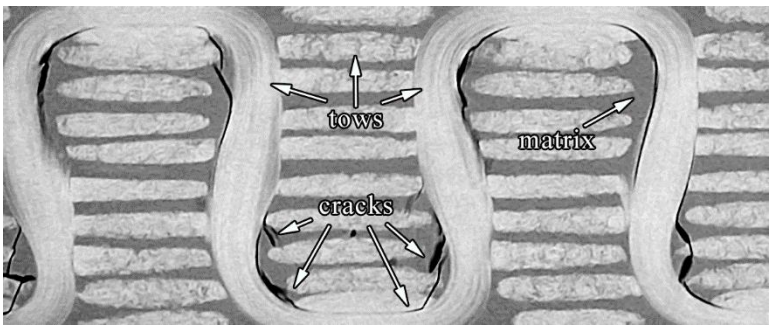

Figure 1. X-ray computed microtomography image of a 3D woven composite with 1x1 orthogonal reinforcement showing microcracks in the matrix due to curing

This paper presents a numerical modeling effort to quantify process-induced residual stresses in 3D woven composites with significant through-thickness constraint and predict initiation of damage in their resin rich areas. We evaluate the applicability of several commonly used failure criteria by comparing the numerically predicted damage with X-ray computed microtomography data. For this purpose, we utilize a realistic finite element model of the one-to-one orthogonally reinforced 3D woven composite on the mesoscale and simulate cooling of the composite after curing. We assume that residual stresses arise solely from the difference in CTEs between carbon fibers and epoxy matrix during the cooling and that chemical shrinkage can be ignored. We utilize the temperature dependent thermo-mechanical properties of the RTM6 epoxy resin reported in [1]. The reinforcement tows are assigned the effective properties of IM7 carbon fiber bundles embedded in resin matrix, see homogenization approaches presented in [2,3] and [4].

The paper is organized as follows. Section 2 presents the four commonly used stress-based failure criteria considered for damage initiation predictions. Section 3 describes our approach to preparation of the mesoscale finite element model and assignment of the temperature-dependent material properties. The results of the simulation of cooling after curing in the absence of damage propagation are given in section 4. In the section, we compare the processing-induced stress concentrations with the damage observed in the X-ray computed microtomography observations performed on actual composite specimens. Section 5 provides predictions of initiation and propagation of damage based on sequential deactivation of elements exceeding the allowable equivalent stress. Section 6 presents the conclusions of this research.

2 DAMAGE INITIATION CRITERIA

We compare the ability of the von Mises, dilatational energy, parabolic and Bauwens criteria to predict initiation of damage in the matrix of a 3D woven carbon/epoxy composite due to residual stresses arising in the material as it cools down from the curing to room temperature. These criteria are formulated as follows.

Von Mises criterion assumes that the material will not yield if the equivalent stress calculated as $\sigma_{VM} = \sqrt{0.5\,[(\sigma_1 - \sigma_2)^2 + (\sigma_1 - \sigma_3)^2 + (\sigma_2 - \sigma_3)^2]}$ is below the critical value:

$$\sigma_{VM} \leq \sigma_{VM}^{crit} \tag{1}$$

where $\sigma_1, \sigma_2, \sigma_3$ are the principal stresses. In our simulations, we use the critical value $\sigma_{VM}^{crit} = 67.8\ MPa$ chosen based on the fracture stress measurements reported in [1].

Dilatational energy criterion is based on the energy required for crack initiation by void nucleation. Assuming linear material behavior, the stress energy density is calculated as

$$U_v = \frac{1-2\nu}{6E}(\sigma_1 + \sigma_2 + \sigma_3)^2 \tag{2}$$

where E is the Young's modulus and ν is the Poisson's ratio of the material. This criterion can be re-written as

$$\sigma_H \leq \sigma_H^{crit}, \tag{3}$$

where $\sigma_H = \frac{1}{3}(\sigma_1 + \sigma_2 + \sigma_3)$ is the hydrostatic stress, and σ_H^{crit} is the value of hydrostatic stress that corresponds to the critical energy density required for cavitation. The approaches to determine this value include the poker chip experiments [5–7], the constrained tube method [8,9] and evaluation of σ_H^{crit} from uniaxial tensile tests [9]. We use the value $\sigma_H^{crit} = 58.7\ MPa$ based on the estimate of $U_v^{crit} = 0.4\ MPa$ for RTM6 epoxy provided in [10].

Parabolic failure criterion was utilized in [11] based on the description provided in [12]. It combines the first and second invariants of stress as

$$\sigma_{VM}^2 + A\,\sigma_H \leq B^{crit} \tag{4}$$

The material parameters A and B^{crit} are found from mechanical testing of the material. Asp et al. [10] provide failure stresses for RTM6 in tension and compression as $\sigma_{yt} = 82\ MPa$ and $\sigma_{yc} = 134\ MPa$. Based on these values we obtain $A = 156\ MPa$, $B^{crit} = 10{,}990\ (MPa)^2$.

Bauwens (Drucker-Prager) criterion uses a linear combination of von Mises and hydrostatic stress to predict failure [12]:

$$\sigma_{VM} + C\ \sigma_H \leq D^{crit} \tag{5}$$

Based on tension and compression results provided in [10], the material parameters are chosen as $C = 0.722$, $D^{crit} = 50.9\ MPa$.

3 GEOMETRIC MODELING AND FINITE ELEMENT MODEL PREPARATION

In this paper we consider an example of the one-to-one orthogonally reinforced composite panel consisting of ten layers of warp and weft tows with a through-thickness binder tow as can be seen, for example, in Figure 1. The panel is 4.1mm thick with in-plane unit cell dimensions of 5.1x5.1mm. The finite element (FE) mesh of the unit cell is generated based on the results of fabric mechanics simulations performed in DFMA software ([13], [14], [15] and later publications by their research group). In the simulations, the user starts with generating an initial pattern of the reinforcement architecture based on the weave pattern, number of yarns, their areas and spacing between. The yarns in the initial pattern (represented by single cylindrical fibers each) are then subdivided into sub-yarns subjected to tensile forces. The relaxation of these forces mimics the weaving process of the 3D woven composites. For better accuracy, the number of sub-yarns is increased and the relaxation process is repeated until the realistic reinforcement geometry is achieved.

The FE mesh of the composite's unit cell (UC) is developed using a custom MATLAB script based on the DFMA results and imported into the commercial FEA software MSC Marc Mentat. Periodic boundary conditions are prescribed on the external lateral surfaces of the composite UC to preserve the material continuity on the macroscale. There is no periodicity in the thickness direction because the entire panel thickness is represented by the UC. All model preparation steps are performed automatically within the MSC Mentat software using a custom Python script. At the completion of script, the user is presented with a ready-to-run model. The details of the DFMA output processing and FEA model preparation can be found in [16,17].

The matrix phase (fully cured HEXCEL RTM6 epoxy resin) is simulated as a linear isotropic material with constant Poisson's ratio $\nu_m = 0.35$, and temperature dependent Young's modulus and thermal expansion coefficient [1]:

$$E_m = E_m^{0℃} - \beta_m T \tag{6}$$

$$\alpha_m = \alpha_m^{0℃} + \gamma_m T \tag{7}$$

where $E_m^{0℃} = 3{,}500\ MPa$, $\beta_m = 5.9 \frac{MPa}{℃}$, $\alpha_m^{0℃} = 5 \cdot 10^{-5} \frac{1}{K}$, $\gamma_m = 1.05 \cdot 10^{-7} \frac{1}{K \cdot ℃}$ are the material parameters, and T is the temperature in $°C$.

The tows consist of 12,000 IM7 carbon fibers impregnated with RTM6 epoxy. The volume fraction of fibers within the tows is set to 80%. Based on the fiber properties provided in [18] and the resin properties $E_m = 2.89\ GPa, \nu_m = 0.35, \alpha_m = 65 \cdot 10^{-6} \frac{1}{K}$ given in Table 2 of [1], the following properties of the tow are obtained: $E_{1t} = 221.38\ GPa, E_{2t} = 13.18\ GPa, G_{12t} = 7.17\ GPa, \nu_{12t} = 0.35, \nu_{23t} = 0.35, \alpha_{1t} = -2.29 \cdot 10^{-7} \frac{1}{K}, \alpha_{2t} = 2.23 \cdot 10^{-5} \frac{1}{K}$. Note that the properties of the matrix in the tows change during curing with temperature, see formulas 6 and 7. However, these changes will result in insignificant variations of the homogenized properties of the tows (0.04% in the longitudinal modulus and 6.5% in the transverse modulus), so in the numerical simulations the properties of the tows are assumed to be temperature independent.

Numerical simulations of cooling after curing of the composite were performed to predict development of the residual stresses during manufacturing process. It was assumed that the material is

fully cured and free of stress in the beginning of the simulation. The UC was assigned a uniform initial temperature distribution of $T_0 = 165\,°C$, and then cooled from curing to room temperature by prescribing a uniform temperature drop of $\Delta T = -140\,°C$ in 40 time increments. The results of the simulations are presented in the next section.

4 PREDICTIONS OF RESIDUAL STRESSES AFTER CURING

Figure 2 presents numerically predicted distributions of the equivalent stresses in the cross-section of the middle of the binder tow perpendicular to the weft direction.

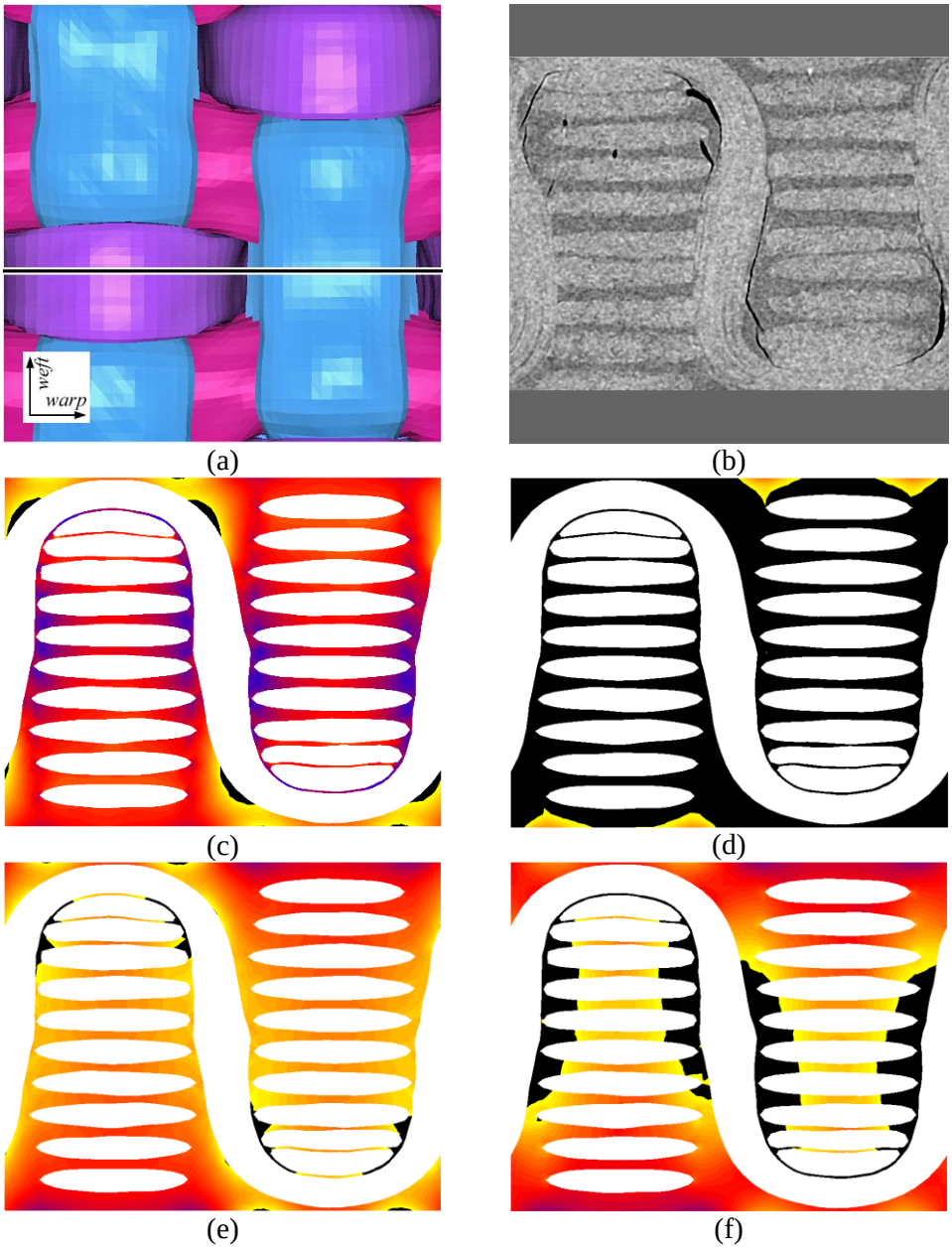

Figure 2. Distribution of the equivalent stresses in the matrix of the UC after cooling: (a) slice location within the UC; (b) microtomography image; (c) von Mises; (d) Bauwens; (e) parabolic criterion with coefficients based on [10]; (f) dilatational energy criterion. The colormap ranges from blue (zero) to yellow with regions above critical value shown in black

It can be seen that von Mises stress criterion (the corresponding distribution is given in panel (c)) predicts damage on the convex surfaces of the binder while the actual composite contains microcracks on the concave sides. It is also evident that Bauwens criterion (panel (d)) significantly overpredicts the extent of damage predicting the entire resin volume to be above the critical value. Both parabolic (panel (e)) and dilatational energy (panel (f)) criteria appear to correctly predict the locations of the damaged regions within the unit cell. It is difficult to make an exact quantitative evaluation – it seems that the actual damaged area is larger than what is predicted by the parabolic criterion, but smaller than what is predicted by the dilatational energy criterion. Note that propagation of damage is not included in this section. It appears that the dilatational energy criterion correlates with the microtomography data better than the other criteria because cracks when formed would alleviate the stress concentrations and limit the extent of further damage to surrounding matrix. This assumption is tested in the next section in which propagation of damage via sequential element deactivation is investigated.

5 PROGRESSIVE DAMAGE MODELING

In this section we model propagation of damage in the composite during cooling after curing via deactivation of the elements exceeding the allowable equivalent stress. Based on the results of the previous section we chose the equivalent stress that corresponds to the dilatational energy criterion. Note that application of the parabolic criterion is presented elsewhere [19]. Due to slower convergence caused by element deactivation 110 increments in the modeling of cooling process from curing to room temperature were used in the simulation.

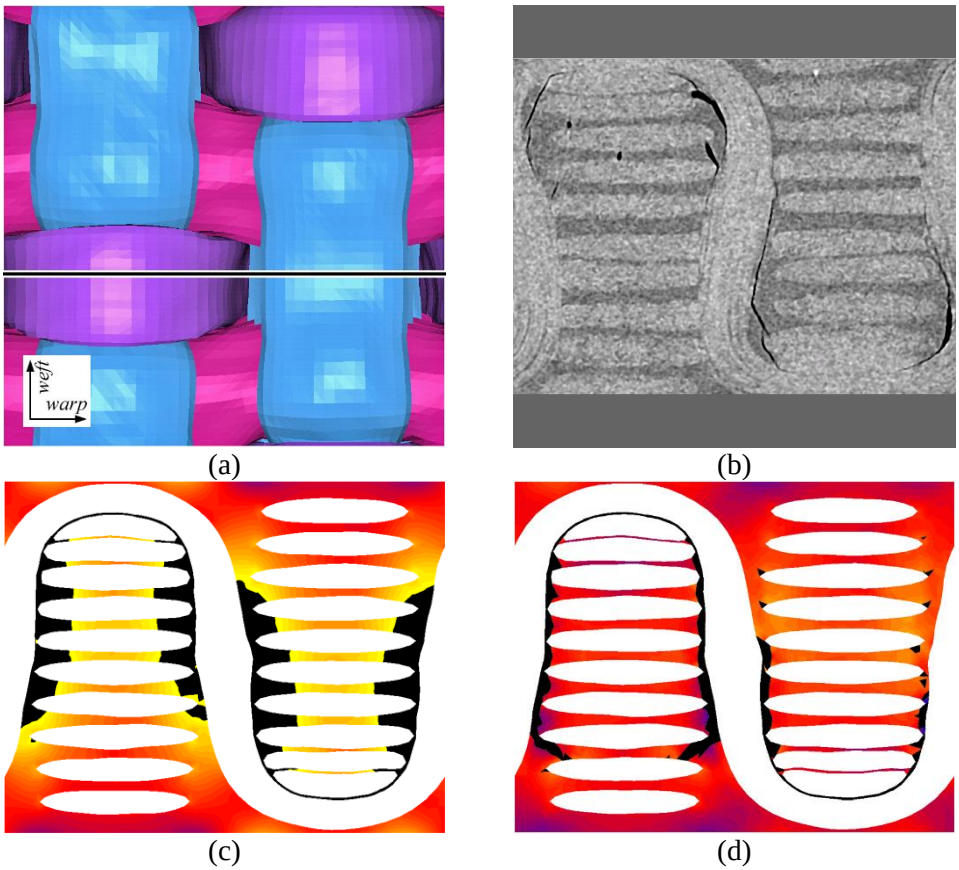

Figure 3. Propagation of damage in the 3D woven composite predicted using the dilatational energy criterion: (a) slice location within the UC; (b) microtomography image; (c) concentrations of the equivalent dilatational stress in uncracked material (areas of stress above critical are shown in black); (d) cracked regions (shown in black) predicted using sequential element deactivation

From the comparison of the stress concentration result (Figure 3c) with the simulation of damage propagation (Figure 3d) it is clear that formation and propagation of the cracks indeed alleviates the residual stresses as was hypothesized earlier. As a result, the final extent of the damage is smaller and more realistic than the one predicted by stress concentration simulations described in section 4.

6 CONCLUSIONS

Meso-scale finite element simulations were performed to predict initiation of processing-induced damage in 3D woven composites due to mismatch in the thermal expansion coefficients between fibers and matrix. Carbon fiber/epoxy resin composite with high level of through-thickness reinforcement (one-to-one orthogonal architecture) was considered because such reinforcement architectures have been shown to develop process-induced microcracks.

The applicability of four commonly used failure criteria – von Mises, parabolic, Bauwens and dilatational energy density – for prediction of processing-induced stress concentration in the matrix of the 3D woven composite was investigated. Comparison of the numerically predicted areas exceeding allowable equivalent stress with X-ray computed microtomography data indicates that the dilatational energy density criterion appears to be the most suitable for analysis of residual stresses leading to microcracking due to mismatch of CTEs during cooling after curing. We simulated damage initiation and propagation via sequential element deactivation based on the dilatational energy criterion. The results of the latter are in good correspondence with microtomography observations.

Our observations indicate that the FEA model presented in this paper can be successfully utilized to predict susceptibility of 3D woven composites to process-induced microcracking. It has the potential of lowering the development costs of new 3D woven architectures by reducing the need for manufacturing of expensive physical prototypes required for studying the microcracking phenomenon.

ACKNOWLEDGEMENTS

This material is based upon work supported by the National Science Foundation through grant CMMI-1100409. We are grateful to Harun Bayraktar and Jon Goering (Albany Engineered Composites, Inc.) for providing the X-ray computed microtomography images of the composites with processing-induced damage and for helpful discussion of the mechanics of 3D woven composites. We acknowledge contribution of Anton Trofimov to the geometric modeling of the composite reinforcement architecture. Financial support from the New Mexico Space Grant Consortium through NASA Cooperative Agreement NNX15AK41A is also gratefully acknowledged.

REFERENCES

[1] C. Brauner, T. Block, H. Purol, A. Herrmann. Microlevel manufacturing process simulation of carbon fiber/epoxy composites to analyze the effect of chemical and thermal induced residual stresses, *Journal of Composite Materials*, **46**, 2012, pp. 2123–2143 (doi:10.1177/0021998311430157).

[2] R.A. Schapery. Thermal Expansion Coefficients of Composite Materials Based on Energy Principles, *Journal of Composite Materials*, **2**, 1968, pp. 380–404 (doi:10.1177/002199836800200308).

[3] Z. Hashin. Analysis of properties of fiber composites with anisotropic constituents, *Journal of Applied Mechanics*, **46**, 1979, pp. 543–550.

[4] I. Tsukrov, M. Giovinazzo, K. Vyshenska, H. Bayraktar, J. Goering, T.S. Gross. Comparison of two approaches to model cure-induced microcracking in three-dimensional woven composites. *Proceedings of the 2012 International Mechanical Engineering Congress & Exposition (IMECE2012)*, Houston, TX: 2012, pp. 1–6.

[5] A.N. Gent, P.B. Lindley. Internal Rupture of Bonded Rubber Cylinders in Tension, *Proceedings of the Royal Society A: Mathematical, Physical and Engineering Sciences*, **249**, 1959, pp. 195–205 (doi:10.1098/rspa.1959.0016).

[6] L.E. Asp, L. Berglund, P. Gudmundson. Effects of a composite-like stress state on the fracture of epoxies, *Composites Science and Technology*, **53**, 1995, pp. 27–37 (doi:10.1016/0266-3538(94)00075-1).

[7] J.W. Kim, G. a. Medvedev, J.M. Caruthers. Observation of yield in triaxial deformation of glassy polymers, *Polymer (United Kingdom)*, **54**, 2013, pp. 2821–2833 (doi:10.1016/j.polymer.2013.03.042).

[8] A. Plepys, M.S. Vratsanos, R.J. Farris. Determination of residual stresses using incremental linear elasticity, *Composite Structures*, **27**, 1994, pp. 51–56 (doi:10.1016/0263-8223(94)90066-3).

[9] T.S. Gross, H. Jafari, J. Kusch, I. Tsukrov, B. Drach, H. Bayraktar, et al. Measuring Failure Stress of RTM6 Epoxy Resin under Purely Hydrostatic Tensile Stress using Constrained Tube Method, *Experimental Techniques*, **41**, 2017, pp. 45–50 (doi:10.1007/s40799-016-0153-2).

[10] L.E. Asp, E. Marklund, J. Varna, R. Olsson. Multiscale modeling of non-crimp fabric composites. *Proceedings of the 2012 International Mechanical Engineering Congress & Exposition (IMECE2012)*, Houston, TX: 2012, pp. 1–10.

[11] T. Hobbiebrunken, M. Hojo, B. Fiedler, M. Tanaka, S. Ochiai, K. Schulte. Thermomechanical Analysis of Micromechanical Formation of Residual Stresses and Initial Matrix Failure in CFRP, *JSME International Journal Series A*, **47**, 2004, pp. 349–356 (doi:10.1299/jsmea.47.349).

[12] L.E. Asp, L.A. Berglund, R. Talreja. A criterion for crack initiation in glassy polymers subjected to a composite-like stress state, *Composites Science and Technology*, **56**, 1996, pp. 1291–1301 (doi:10.1016/S0266-3538(96)00090-5).

[13] Y. Wang, X. Sun. Digital-element simulation of textile processes, *Composites Science and Technology*, **61**, 2001, pp. 311–319 (doi:10.1016/S0266-3538(00)00223-2).

[14] G. Zhou, X. Sun, Y. Wang. Multi-chain digital element analysis in textile mechanics, *Composites Science and Technology*, **64**, 2004, pp. 239–244 (doi:10.1016/S0266-3538(03)00258-6).

[15] Y. Miao, E. Zhou, Y. Wang, B. Cheeseman. Mechanics of textile composites: Micro-geometry, *Composites Science and Technology*, **68**, 2008, pp. 1671–1678 (doi:10.1016/j.compscitech.2008.02.018).

[16] A. Drach, B. Drach, I. Tsukrov. Processing of fiber architecture data for finite element modeling of 3D woven composites, *Advances in Engineering Software*, **72**, 2014, pp. 18–27 (doi:10.1016/j.advengsoft.2013.06.006).

[17] B. Drach, A. Drach, I. Tsukrov, M. Penverne, Y. Lapusta. Finite Element Models of 3D Woven Composites Based on Numerically Generated Micro-Geometry of Reinforcement. *Proceedings of the American Society for Composites 2014 - 29th Technical Conference on Composite Materials*, San Diego, CA: 2014.

[18] I. Tsukrov, H. Bayraktar, M. Giovinazzo, J. Goering, T.S. Gross, M. Fruscello, et al. Finite Element Modeling to Predict Cure-Induced Microcracking in Three-Dimensional Woven Composites, *International Journal of Fracture*, **172**, 2011, pp. 209–216 (doi:10.1007/s10704-011-9659-x).

[19] D. Kuksenko, B. Drach, I. Tsukrov. Prediction of Damage Initiation and Simulation of Damage Propagation in 3D Woven Composites during Processing. *Proceedings of the American Society for Composites - 32nd Technical Conference, ASC 2017*, West Lafayette, IN, USA: 2017.